

Robust Cooperative Localization in a dynamic environment Using Factor Graphs and Probability Data Association Filter

Dhiraj Gulati^{*§}, Feihu Zhang[†], Daniel Malovetz^{*}, Daniel Clarke[‡] and Alois Knoll[§]

^{*}fortiss GmbH, München, Germany. {gulati, malovetz}@fortiss.org

[†]School of Marine Science and Technology, Northwestern Polytechnical University, 710072, Xi'an, China. feihu.zhang@nwpu.edu.cn

[‡]Cogsense Technologies Limited, United Kingdom. daniel.clarke@cogsense.co.uk

[§]Technische Universität München, Garching bei München, Germany. dhiraj.gulati@tum.de, knoll@in.tum.de

Abstract—Autonomous vehicles operating in dynamic environments rely on precise localization. In this paper we present a novel approach for cooperative localization of vehicular systems and an infrastructure RADAR which is resilient against outliers generated from the RADAR. The problem of cooperative localization is represented as a factor graph, where interrelated topologies (including that of outliers) are added as constraint factor between vehicle states. Corresponding probabilities for multiple topologies between states of the two vehicles are calculated using the Probability Data Association Filter and assigned to the respective edges in the graph. Simulation results indicate that this technique has significant benefits in the context of improving the resilience against outliers while optimizing joint state estimates. The methodology presented in this paper has the potential to provide a robust and flexible framework for cooperative localization in the presence of clutter, obscuration and targets entering and leaving the field of view.

I. INTRODUCTION

With advancements in communication technologies and increase in the sensor proliferation in the environment, Cooperative Localization (CL) has become a viable and beneficial solution for a number of autonomous vehicles [1].

Many solutions use the Kalman Filter (or its derivatives like Extended Kalman Filter and Unscented Kalman Filter) [2] for tracking the cooperative state variables and their covariances. Other methodologies like Markov Localization [3], split covariance intersection filter [4], random finite set framework [5], and Symmetric Measurement Equation Filter [6] also provide novel ways of solving this problem.

The CL problem can also be formulated and solved as a graph. Pose graph and Landmark SLAM (Simultaneous Localization and Mapping) is one of the commonly used methods. GTSAM [7] and g^2o [8] are examples two such frameworks which provide various graph based estimates based on SLAM for robotic use. Graph based solutions easily adapted for non linear problems and hence are at times well suited for real world problems.

Our previous work ([9]) proposed a solution which added a Topology Factor into the graphical model, implemented as a factor graph in the GTSAM framework. By incorporating additional information (through the Topology Factor),

improved performance over the Kalman Filter was achieved. This work also addressed other challenges, namely bandwidth limitations; data association uncertainties; unknown coordinate transformations; and scalability.

This paper proposes a novel method for providing robust CL when the configuration of external sensor (here RADAR) is unknown. Although quite accurate, RADAR generates a significant clutter. But [9] assumes a clutter free environment. Therefore the proposed solution in [9] can result in multiple topology constraints between the states of vehicles. The key idea presented herein is to track and assign probabilities to these topological constraints between targets. Optimization algorithms (e.g. Gauss Newton or Levenberg Marquardt) are used to optimize the joint probability density function and extract the final fused states. The topology resulting from the clutter will get a lower probability and hence, will have less weight when trying to solve the problem graph. The performed experiments show high resilience to clutter detected by the RADAR.

This problem can also be generalized for any solution which uses a graph based framework. Sünderhauf et al. [10] proposed the method of Switchable Constraints which strengthens the pose graph based solution specifically against false loop closures. Instead of incorporating another data association algorithm in parallel to SLAM, the solution rejects the outliers during the optimization.

II. PROBLEM DESCRIPTION

A simple CL scenario can be seen in the Fig. 1(a). Dotted blue lines represent the RADAR coordinate system.

The assumptions are as follows:

- 1) Vehicles have GPS sensors to measure their position in an absolute reference of a 2D global coordinate system.
- 2) The infrastructure RADAR sensor measures the relative positions of the vehicles in its own local 2D coordinate system. Its configuration information is not available, such that its location and orientation is unknown.

- 3) The vehicles and the RADAR Sensor can communicate in either direction to exchange data. There is no timing delay or data error in communication.
- 4) No mechanism is available, including communication mechanism and/or the protocol to identify individual vehicles. This introduces a challenge from the perspective of data association.
- 5) The environment has uniform clutter and can have miss detections.

Then the task of CL is to lower the error in position estimation by fusing the measurements from all the sensors.

III. FACTOR GRAPHS

A. Overview

Definition: A bipartite graph $G_k = (F_k, V_k, E_k)$ is defined as a Factor Graph when: (1) It has two types of nodes: factor nodes $f_i \in F_k$ and variable nodes $v_j \in V_k$; (2) Edges $e_{ij} \in E_k$ can exist only between factor nodes and variable nodes, and are present if and only if the factor f_i involves a variable v_j [11].

In simpler words, a factor graph explains the connection between the complex functions and its factors of simpler functions. Fig. 1(b) shows a simple factor graph with variables a, b, c, d, e and functions f_1 and f_2 with factorization: $h(a, b, c, d, e) = f_1(a, b, c) * f_2(c, d, e)$.

Factor graphs were initially introduced for the calculation of the sum-product algorithm [12]. Indelman, V. et al. [11] demonstrated the use of factor graph for multi-sensor information fusion for navigation.

B. Factor Graph formulations

A factor graph G_k (using the above definition) can be expressed as:

$$g(X) = \prod_i f_i(X_i), \quad (1)$$

where X_i is the set of all variables x_j connected by an edge to factor f_i .

An error function of each factor f_i represents the error between the predicted measurement and the actual measurement. To obtain the predicted state, the aim for non-linear least

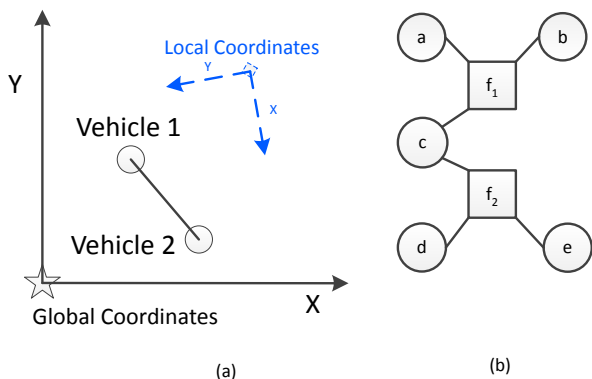


Fig. 1. (a) Topology for vehicle infrastructure CL. Dashed Axis in blue represent the coordinate system of the RADAR. (b) Factor graph with variables a, b, c, d, e and functions $f_1(a, b, c)$ and $f_2(c, d, e)$.

squares optimizers is to minimize this function. This is done by adjusting the estimates of the variables X . The optimal estimate \hat{X} for complete graph G is obtained as:

$$\hat{X} = \arg \min_X \left(\prod f_i(X_i) \right) \quad (2)$$

The above methodology can be compared with Kalman Filter. $h(\cdot)$ is the measurement model that predicts a sensor measurement from a given state estimate. The factor is then synonymous with this measurement model. For a Gaussian noise model, a measurement factor can be written as:

$$f_i(X_i) = d[h_i(X_i) - z_i], \quad (3)$$

where $h_i(X_i)$ is the measurement model as a function of the state variables X_i ; z_i is the actual measurement and the operator $d(\cdot)$ represents a cost function.

The process model can be similarly represented as a factor graph (more detail is provided in [13]).

C. Factor formulations

We briefly explain how factors are generated for various sensor measurements. For details, please check [9].

1) *Odometry Measurements:* Using a constant velocity model, the odometry measurement equation is given by:

$$z_{t+1}^o = h^o(z_t^o) + n^o \quad (4)$$

where z_t^o is the Odometry measurement at time t , h^o is the function to calculate the odometry measurement at time $t+1$ and n^o is the measurement noise. This results in a binary factor, f^{ODOM} , and for states X_{t+1}, X_t can be written as:

$$f^{ODOM}(X_{t+1}, X_t) \triangleq d(z_{t+1}^o - h^o(z_t^o)) \quad (5)$$

2) *GPS Measurements:* The GPS measurement equation is:

$$z_t^g = h^g(z_t) + n^g, \quad (6)$$

where n^g is the measurement noise and h^g is the measurement function, providing the relation between the measurement z_t^g and the position of the vehicle. Equation (6) gives an unary factor f^{GPS} which is written as:

$$f^{GPS}(X_t) \triangleq d(z_t^g - h^g(z_t)) \quad (7)$$

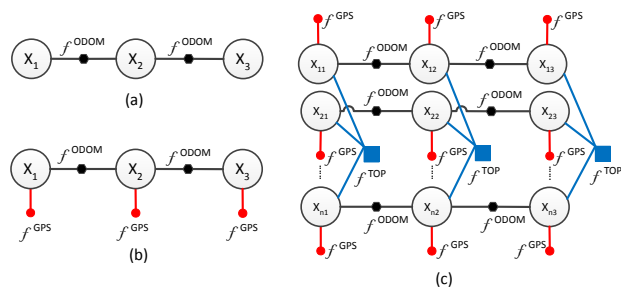


Fig. 2. (a) Factor graph with three state nodes and two odometry factors. (b) Factor graph with three state nodes, two odometry factors and three GPS factors. (c) Factor graph for n vehicles with three state nodes, two odometry factors, three GPS factors and two topology factors each.

3) *Topology Measurements*: The topology information (the inter-vehicle distance) at time t can be calculated as:

$$(z_t^T)^2 = \sum_{i=1}^{N-1} \sum_{j=i+1}^N (p_{x,t}^i - p_{x,t}^j)^2 + \sum_{i=1}^{N-1} \sum_{j=i+1}^N (p_{y,t}^i - p_{y,t}^j)^2 \quad (8)$$

where $p_{x,t}^i, p_{y,t}^i$ represents the x and y position of i^{th} vehicle as observed by RADAR. p^j terms are analogous to p^i terms. This can be formulated as following:

$$(z_t^T)^2 = h^{top}(z^1, \dots, z^N) + n^{top} \quad (9)$$

where n^{top} is the measurement noise, $z^i = (p_x^i, p_y^i)$ and h^{top} is the new measurement function, relating between measured positions of all the N vehicles and the new topology measurement. The corresponding $N - ary$ factor, for N vehicles, becomes:

$$f^{TOP}(X_{1t}, \dots, X_{Nt}) \triangleq d((z_t^T)^2 - h^{top}(z^1, \dots, z^N)) \quad (10)$$

Fig. 2 illustrates Factor Graphs with various factors.

D. Smoothing

We use the LM optimization algorithm to solve the factor graph. Using an initial estimate x_0 it iteratively finds an update Δ from the linearized system:

$$\arg \min_{\Delta} J(x_0)\Delta - b(x_0) \quad (11)$$

where $J(x_0)$ is the sparse Jacobian Matrix at the current linearization point x_0 and $b(x_0) = h(x_0) - z$ is the residual for given the measurement z . The Jacobian matrix is equivalent to a linearized version of the factor graph, and its block structure reflects the structure of the factor graph. After solving (11), the linearization point is updated to the new estimate $x_0 + \Delta$. Further detail on this process is presented within [11].

The Jacobian for the Odometry, calculated from (4), is $\text{diag}[1, 1]$. Further detail on this process is presented in [9]. The Jacobian for GPS from (6) is same as that of odometry.

The Jacobian for topology measurement from (8) with ∂x and ∂y is:

$$\text{diag} \left[\sum_{i=1}^{N-1} \sum_{j=i+1}^N 2 * (p_{x,t}^i - p_{x,t}^j), \sum_{i=1}^{N-1} \sum_{j=i+1}^N 2 * (p_{y,t}^i - p_{y,t}^j) \right] \quad (12)$$

E. Topology Measurement Uncertainties/Covariances

Odometry and GPS sensors provide the measurements directly and their uncertainties/covariances are provided by sensor manufacturers. The topology measurement is a derived measurement. If σ_x^2 and σ_y^2 are the x and y variances respectively for the infrastructure sensor (refer [14] for details), then we get:

$$\text{Cov}(x, y) = \text{diag} [\sigma_{x_1}^2, \dots, \sigma_{x_n}^2, \sigma_{y_1}^2, \dots, \sigma_{y_n}^2] \quad (13)$$

Then using (8) and (13), we obtain the covariance for the topology estimate at any time t as:

$$\sigma_{top_{x,y}}^2 = M \cdot \text{Cov}(x, y) \cdot M^T \quad (14)$$

where M is a $1 \times 2N$ matrix as follows:

$$M = \left[\frac{\partial}{\partial x_1} (z_t^T)^2, \dots, \frac{\partial}{\partial x_n} (z_t^T)^2, \frac{\partial}{\partial y_1} (z_t^T)^2, \dots, \frac{\partial}{\partial y_n} (z_t^T)^2 \right] \quad (15)$$

IV. PROBABILITY DATA ASSOCIATION FILTER

Probability Data Association Filter (PDAF) is a well known Bayesian target tracking filter. Instead of using one measurement to update the state, it utilizes all the measurements of the target. It discards the measurements which do not satisfy the given limits, known as Gates, and assigns weights to the remaining validated ones [15].

Here we give only a brief overview of calculating the probabilities of multiple measurements at any given time. Please refer to [16] for details.

Let z_t be the set of validated multiple observations at time t and let m_t be the number of observations at time t . Then we get:

$$z_t = \{z_t^1, \dots, z_t^{m_t}\} = \{z_t^i\}_{i=1}^{m_t} \quad (16)$$

And the complete set of observations up to time t as

$$Z_t = \{z_j\}_{j=1}^t \quad (17)$$

Using the above defined sets of observations, lets us define the following events:

$$\begin{aligned} \chi_t^i &= \{z_t^i \text{ is the correct measurement}\}, i = 1, \dots, m_t \\ \chi_t^0 &= \{\text{None of the validated measurement is correct}\} \end{aligned} \quad (18)$$

Using (18) and (17), we define β_t^i , a posteriori probability of each return having originated from the object in track as:

$$\beta_t^i \triangleq P\{\chi_t^i | Z_t\}, i = 0, 1 \dots, m_t \quad (19)$$

This is the 'probabilistic data association'.

Now \hat{x}_t , the final state estimate at time t , using β_t^i can be written as:

$$\hat{x}_t = \sum_{i=0}^{m_t} \hat{x}_t^i \beta_t^i \quad (20)$$

where \hat{x}_t^i denotes the updated state conditioned on χ_t^i .

The association probabilities for the set z_t are then calculated as

$$\beta_t^i = \frac{e_i}{\sum_{i=0}^{m_t} e_i}, \quad (21)$$

where,

$$e_i = \exp \left(-\frac{1}{2} (\tilde{z}_t^i)^T S_t^{-1} \tilde{z}_t^i \right), i = 1, \dots, m_t \quad (22)$$

$$e_0 = (2\pi/\gamma)^{n_z/2} m_t c_{n_z} (1 - P_D P_G) / P_D \quad (23)$$

where S_t , P_G and P_D denote the innovation covariance, the generation probability (the target originated measurement falls within the validation gate) and the detection probability (the correct measurement is detected) respectively. \tilde{z}_t^i denotes the innovation. c_{n_z} is the volume of the n_z dimensional unit hypersphere ($c_1 = 2, c_2 = \pi, c_3 = 4\pi/3, \text{etc.}$). γ is the

threshold for the validated measurements by defining the following validation region:

$$\{z^i : (z_t^i)^T S_t^{-1} z_t^i \leq \gamma\} \quad (24)$$

Hence using PDA filter, it is possible to calculate the association probability β_t^i for each validated radar measurement z^i at time t , and false-positive measurements are later assigned with lower weights.

V. SOLUTION

To solve the problem presented in Section II, we implement the PDA Filter along side the Factor Graph. The probabilities thus obtained from the PDA Filter are used as the weights for the factors.

Measurement factor in eq. (3) contributes fully while trying to estimate the corresponding state. For a total of m_i measurements (including clutter) for a state, each with some probability, the measurement factor can be rewritten as:

$$f_i(X_i) = \beta_i^j \cdot d[h_i(X_i) - z_i], j = 1, \dots, m_i \quad (25)$$

where β_i^j is the probability for j^{th} measurement of i^{th} state.

RADAR measurements are often accompanied with some clutter. Hence we track the topology of the vehicles. Using (25) and (10), we get:

$$f^{TOP}(X_{1t}, \dots, X_{Nt}) \triangleq \beta_i^j \cdot d((z_t^T)^2 - h^{top}(z^1, \dots, z^N)) \quad (26)$$

where β_i^j is the probability for j^{th} measurement of i^{th} state.

The solution can be understood from Fig. 3. RADAR results in three measurements (represented with triangles) for the first vehicle and one for the second vehicle for $(n-1)^{\text{th}}$ state. For the n^{th} state corresponding measurements are two and three respectively. Of these multiple measurements for each state only one is the true measurement and rest are clutter. Each RADAR measurement is represented by a triangle of different colour.

Now three measurements of the first vehicle and one measurement of the second vehicle at $(n-1)^{\text{th}}$ give us three topology factors. These are represented by the squares. Similarly it gives six topology factors for the n^{th} state. Our proposed solution works as follows. The dotted circle represents the Gate for the topology measurements, i.e. the topology factors which satisfies the Gate are considered and rest are removed. For each of the validated measurement probability is calculated using PDAF. In the figure the size of the rectangle inside the Gate represents the probability of the measurement. These calculated probabilities are used in (26). Hence only validated topology factors contribute to the final solution based on the weights.

VI. EVALUATION

A. System Setup

The simulation was implemented with two vehicles on a ground plane for 200 steps. To implement the factor graphs and the corresponding factors we utilize the Georgia Tech smoothing and Mapping (GTSAM) open source library [7].

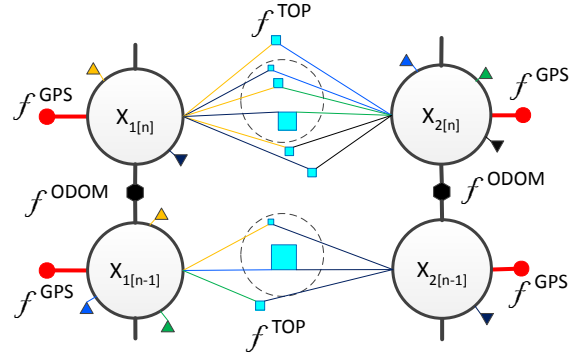


Fig. 3. Factor graph for $(n-1)$ and n^{th} state of two vehicles with four state nodes, two Odometry factors, four GPS factors and nine topology factors. Dotted circle represents Gate Boundary for PDA Filter. Triangles represent the RADAR readings of the vehicles associated with the states.

Simulated vehicles have internal sensors to measure their location in global coordinates. A RADAR sensor is assumed to be located outside the two simulated vehicles, and provides location within its local coordinate system. No configuration information for the RADAR is available and hence the transformation between the two coordinate systems is unknown.

All the sensors are assumed to have zero mean Gaussian noise. The covariances are assumed as $\text{diag}[1.0, 1.0]$ and $\text{diag}[15.0, 15.0]$ for the Odometry and the GPS respectively. We assume the step interval T as 1. The RADAR has one valid reading with covariance $\text{diag}[0.5, 0.5]$ and the remaining is clutter having uniform distribution. For our tests we randomly generate 1-3 measurements for each vehicle, resulting in a maximum of 9 Topology Factors between two vehicles at each time step.

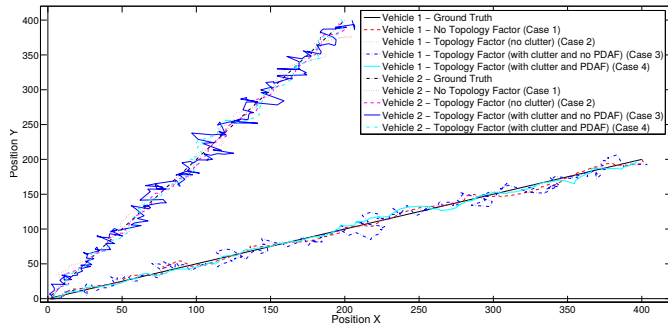
For tracking the topology factor, PDAF has the detection probability and generation probability of 0.99. We assume the corresponding track detection and initialization has been already successful. Then using PDAF we assign the probabilities to the resulting topologies for a given state.

The performance is measured by calculating Root Mean Square Deviation (RMSE) value for the complete system.

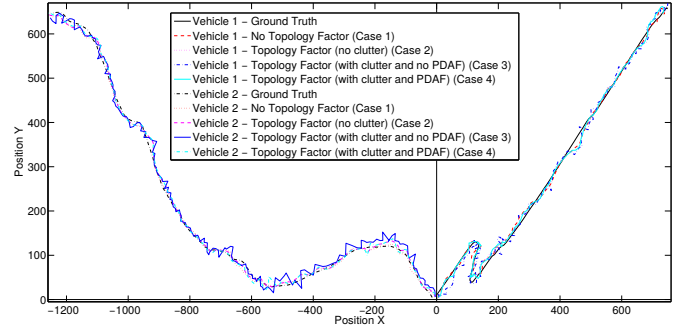
We perform the simulation, and compare and contrast our results four way, between:

- 1) the fused trajectory only using Odometry and GPS measurements.
- 2) the fused trajectory for Odometry, GPS measurements and Topology Factor with probability 1 for each state (assuming no clutter).
- 3) the fused trajectory for Odometry, GPS measurements and multiple Topology Factors for each state (assuming clutter) with probability 1 assigned to each of them. This implies we incorporate all the Topology Factors resulting from RADAR.
- 4) the fused trajectory for Odometry, GPS measurements and multiple Topology Factors for each state (assuming clutter) with probability assigned to each of them using PDAF (proposed solution).

We perform two such simulations, one set with linear trajectories and the second with random trajectories.

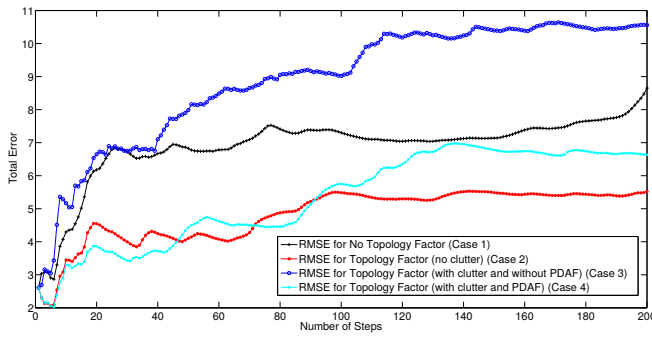


(a)

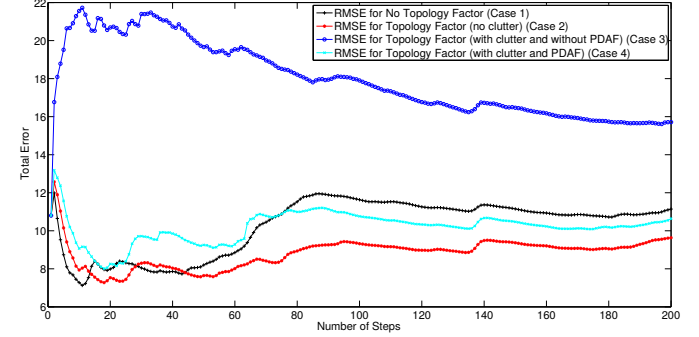


(b)

Fig. 4. Ground Truth and fused trajectories for two vehicle simulation. Case 2 without clutter (unrealistic scenario) and with topology, results in the trajectory near to the Ground Truth. Case 3 with clutter (realistic scenario) includes all clutter measurements from RADAR and with topology, results in the worst trajectory. Case 4 with clutter (realistic scenario) assigned weights using a PDAF and with topology, although is worse than Case 2, results in a better trajectory than the Case 3 which is a realistic scenario and Case 1 (which does not use any topology).

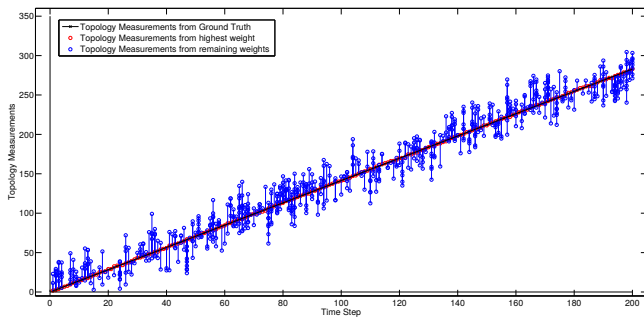


(a)

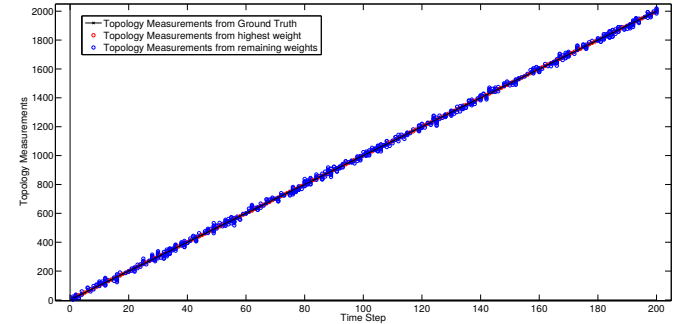


(b)

Fig. 5. RMSE for two vehicle simulation. Case 2 without clutter (unrealistic scenario) and with topology, has the least error. Case 3 with clutter (realistic scenario) includes all clutter measurements from RADAR and with topology, has the maximum error. Case 4 with clutter (realistic scenario) assigned weights using a PDAF and with topology, although has more error than Case 2, but performs better than Case 3 which a realistic scenario and Case 1 (which does not use any topology).



(a)



(b)

Fig. 6. Topology Measurements for 200 steps (refer Results).

B. Results

Fig. 4(a) and 4(b) shows the ground truth, and the trajectories from the four methods for 2 vehicles. It can be seen that trajectory for the proposed approach (Case 4) is close to the ground truth and performs better than no topology (Case 1). But it performs little worse when compared to the Case 2 where it uses only one measurement with probability 1. But the Case 2 also assumes no clutter which is untrue in real

environments. And if we use all the measurements (including clutter) from the RADAR (Case 3), the trajectory is the worst.

This can be further verified quantitatively and qualitatively by the total RMSE values of the system as plotted in graphs in Fig. 5(a) and 5(b) for Fig. 4(a) and 4(b) respectively. RMSE for the Case 3 (with clutter and without PDAF) is even higher than the Case 1 of no topology factor. This is because clutter significantly increases the error by adding false information to

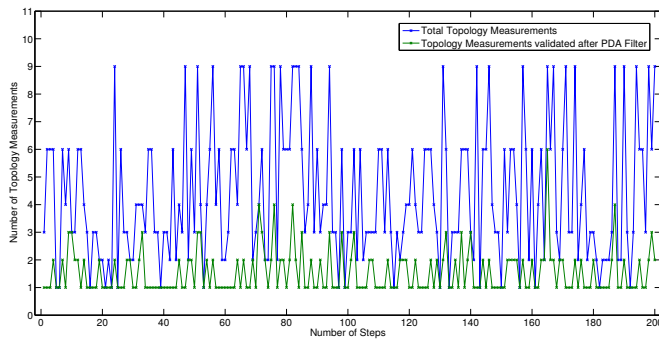


Fig. 7. Comparison of validated measurements by PDA Filter and the total measurements for Fig. 4(a) (refer Results).

the graph. Although the Case 2 (without clutter) performs the best (as it does not add any false information to the problem graph) but does not reflect the real environment. Hence it can be seen from RMSE using PDAF with cluttered measurements (Case 4) is an effective solution for the real environments.

Fig. 6(a) and 6(b) show the plot of topology measurements for Fig. 4(a) and 4(b) respectively. Since topology measurements is a one dimension value, all the measurements for a step fall on a straight line parallel to Y-axis.

Fig. 7 compares the the total topology measurements for all the steps against the topology measurements selected by PDA Filter, which are effectively used by the LM Algorithm for estimating the final states for Fig. 4(a).

C. Remarks

Presently, the solution is implemented as a batch process. A online solution like iSAM2 of GTSAM can be used for run-time state estimation. Further it also has the potential of supporting plug-and-play paradigm [17].

The results presented here assume tracking of two vehicle system, thereby resulting in one topology measurement which can be tracked using PDA Filter. For more than two vehicles we would need Joint Probability Data Association Filter (JPDA) [18]. Therefore further work should evaluate the robustness of the solution with multiple vehicle systems.

VII. CONCLUSION

False positive measurements are Achilles' heel for graph based solutions. The burden of correct graph construction falls on a separate front end module. This front end heavily relies on input from sensors, which inherently have a certain degree of unreliability and can also result in clutter measurements. The PDA filter alongside the factor graph implementation results in a solution which can provide resilience against such clutter, that may have escaped the initial front end filtering. Simulation results indicate that, the presence of clutter for a graph with weighted Topology Factors does degrade the RMSE performance when compared against situation with only Topology Factors and no clutter. But important result is that, RMSE of the proposed solution is still superior than the case without any topological factor. Therefore, this has a potential to solve the challenge of cooperative localization in realistic dynamic

scenarios where (1) location and configuration of RADAR is unknown; and (2) clutter, obscuration and miss detections degrade the state estimates.

Future work will focus on the presented approach for more than two vehicle systems with incremental smoothing using real data.

ACKNOWLEDGMENT

This work was supported by fortiss GmbH and BMWi IKT III SADA Project <http://www.projekt-sada.de/>.

REFERENCES

- [1] R. Kurazume, S. Nagata, and S. Hirose, "Cooperative positioning with multiple robots," in *Robotics and Automation, 1994. Proceedings., 1994 IEEE International Conference on*, May 1994, pp. 1250–1257 vol.2.
- [2] S. I. Roumeliotis and G. A. Bekey, "Distributed multirobot localization," *IEEE Transactions on Robotics and Automation*, vol. 18, no. 5, pp. 781–795, Oct 2002.
- [3] D. Fox, W. Burgard, H. Kruppa, and S. Thrun, "A probabilistic approach to collaborative multi-robot localization," *Autonomous robots*, vol. 8, no. 3, pp. 325–344, 2000.
- [4] H. Li and F. Nashashibi, "Cooperative multi-vehicle localization using split covariance intersection filter," *IEEE Intelligent Transportation Systems Magazine*, vol. 5, no. 2, pp. 33–44, Summer 2013.
- [5] F. Zhang, H. Stähle, G. Chen, C. Buckl, and A. Knoll, "Multiple vehicle cooperative localization under random finite set framework," in *2013 IEEE/RSJ International Conference on Intelligent Robots and Systems*, Nov 2013, pp. 1405–1411.
- [6] E. W. Kamen, "Multiple target tracking based on symmetric measurement equations," *IEEE Transactions on Automatic Control*, vol. 37, no. 3, pp. 371–374, Mar 1992.
- [7] "GTSAM, Georgia Tech smoothing and Mapping," <https://collab.cc.gatech.edu/borg/gtsam/>.
- [8] R. Kümmerle, G. Grisetti, H. Strasdat, K. Konolige, and W. Burgard, "G2o: A general framework for graph optimization," in *Robotics and Automation (ICRA), 2011 IEEE International Conference on*, May 2011, pp. 3607–3613.
- [9] D. Gulati, F. Zhang, D. Clarke, and A. Knoll, "Vehicle infrastructure cooperative localization using factor graphs," in *2016 IEEE Intelligent Vehicles Symposium (IV)*, June 2016, pp. 1085–1090.
- [10] N. Sinderhauf and P. Protzel, "Switchable constraints for robust pose graph slam," in *2012 IEEE/RSJ International Conference on Intelligent Robots and Systems*, Oct 2012, pp. 1879–1884.
- [11] V. Indelman, S. Williams, M. Kaess, and F. Dellaert, "Factor graph based incremental smoothing in inertial navigation systems," in *Information Fusion (FUSION), 2012 15th International Conference on*, July 2012, pp. 2154–2161.
- [12] F. R. Kschischang, B. J. Frey, and H. A. Loeliger, "Factor graphs and the sum-product algorithm," *IEEE Transactions on Information Theory*, vol. 47, no. 2, pp. 498–519, Feb 2001.
- [13] F. Dellaert and M. Kaess, "Square root sam: Simultaneous localization and mapping via square root information smoothing," *Int. J. Rob. Res.*, vol. 25, no. 12, pp. 1181–1203, Dec. 2006. [Online]. Available: <http://dx.doi.org/10.1177/0278364906072768>
- [14] K. O. Arras, "An introduction to error propagation: Derivation, meaning and examples of $cy = fx \ cx \ fx$," Tech. Rep., 1998.
- [15] Y. Bar-Shalom, F. Daum, and J. Huang, "The probabilistic data association filter," *IEEE Control Systems*, vol. 29, no. 6, pp. 82–100, Dec 2009.
- [16] Y. Bar-Shalom and E. Tse, "Tracking in a cluttered environment with probabilistic data association," *Automatica*, vol. 11, no. 5, pp. 451–460, 1975.
- [17] H. P. Chiu, X. S. Zhou, L. Carlone, F. Dellaert, S. Samarasekera, and R. Kumar, "Constrained optimal selection for multi-sensor robot navigation using plug-and-play factor graphs," in *2014 IEEE International Conference on Robotics and Automation (ICRA)*, May 2014, pp. 663–670.
- [18] T. E. Fortmann, Y. Bar-Shalom, and M. Scheffe, "Multi-target tracking using joint probabilistic data association," in *Decision and Control including the Symposium on Adaptive Processes, 1980 19th IEEE Conference on*, Dec 1980, pp. 807–812.